

## Surface-structure determinations by means of off-normal photoelectron diffraction: A kinematical analysis

E. L. Bullock, C. S. Fadley, and P. J. Orders\*

Department of Chemistry, University of Hawaii, Honolulu, Hawaii 96822

(Received 25 July 1983)

Recent off-normal photoelectron diffraction data of Barton *et al.* for  $c(2 \times 2)S$  on Ni(001) and  $p(2 \times 2)S$  on Cu(001) are analyzed using a single-scattering cluster model. The  $\chi(E)$  curves and their Fourier transforms (FT's) are sufficiently well predicted by this model to permit a detailed analysis of the origins of the FT peaks. No simple connection of these peaks with single nearest-neighbor substrate path-length differences is possible, in contrast with a prior analysis of the same data.

In several prior studies,<sup>1-3</sup> adsorbate core-level photoelectron diffraction (PD), in which the experimental geometry is fixed while the photon energy is scanned, has been used to derive surface atomic geometries. Two distinct geometries have been utilized: normal-emission (NPD) and off-normal emission (OPD). In determining structures, the resulting extended x-ray absorption fine-structure-like oscillations in a normalized  $\chi(E)$  intensity curve are compared with a series of multiple-scattering calculations,<sup>1,2</sup> and/or Fourier transformed to yield what has been suggested to be more direct geometrical information.<sup>1-3</sup> However, it has been pointed out<sup>4</sup> that a single-scattering cluster (SSC) model provides a good description of NPD data, and that the peaks found in Fourier transforms of such data are generally associated with several path-length differences (PLD's) for various strong atomic scatterers in the cluster. Thus it will generally be difficult to derive vertical interplanar distances or bond lengths directly from such NPD Fourier transforms.<sup>4</sup>

In a very recent study, Barton *et al.*<sup>3</sup> have obtained experimental OPD curves for S 1s emission from both  $c(2 \times 2)S$  on Ni(001) (a well-defined test case known to be fourfold

bonded at a vertical distance of  $z = 1.30-1.40 \text{ \AA}$ ) (Ref. 5) and  $p(2 \times 2)S$  on Cu(001) (a case for which the bonding geometry is not known). The experimental geometries chosen are indicated in Fig. 1, together with various important atomic scatterers. The angle  $\theta_{e^-} = 45^\circ$ , so that electron emission is fixed along [110] for both cases;  $\theta_{h\nu} = 45^\circ$  for S on Ni, so that the polarization vector  $\hat{\epsilon}$  is directly along the emission direction; and  $\theta_{h\nu} = 30^\circ$  for S on Cu, so that  $\hat{\epsilon}$  has a larger component parallel to the surface. For Ni, this geometry should emphasize direct backscattering from the nearest-neighbor Ni labeled "1" because the polarization-dependent photoelectric matrix element will preferentially direct the primary wave toward this atom. The experimental results for S on Ni for both  $\chi(E)$  and its autoregressive Fourier transform (FT) are shown in the uppermost panels of Figs. 2 and 3.<sup>3</sup> Barton *et al.* have interpreted the peaks

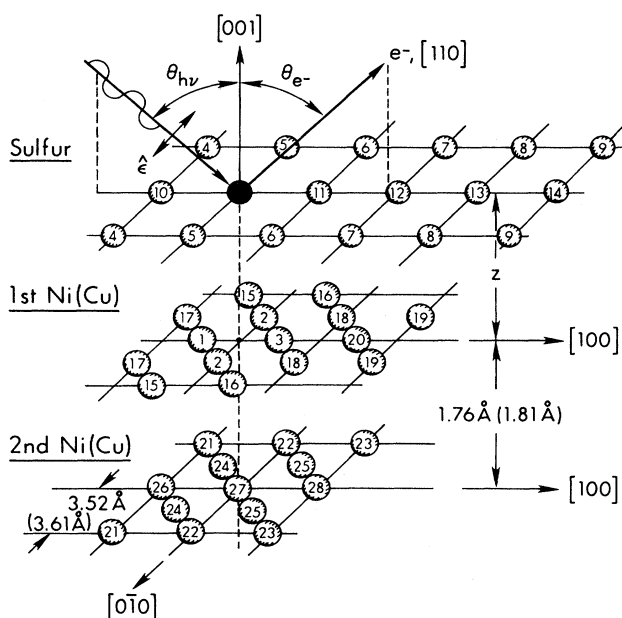


FIG. 1. Experimental geometry, with various potentially important S and Ni (or Cu) scatterers shown. Mirror symmetry dictates two atoms of type  $S_4$ ,  $Ni_2$ ,  $Ni_{24}$ , etc.

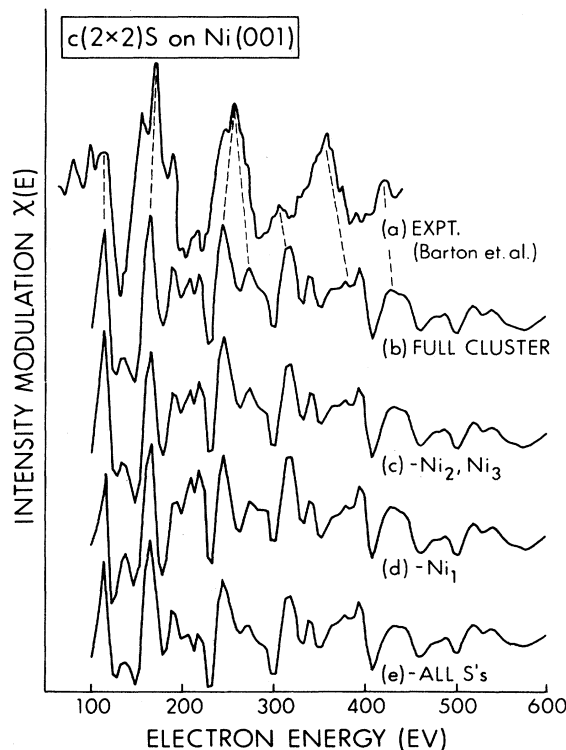


FIG. 2. OPD  $\chi(E)$  curves for  $c(2 \times 2)S$  on Ni(001): (a) experimental data of Barton *et al.* (Ref. 3); (b) full-cluster SSC theory; (c) full cluster minus  $Ni_2$  and  $Ni_3$  atoms; (d) full cluster minus  $Ni_1$  atom; and (e) full cluster minus all S atoms.

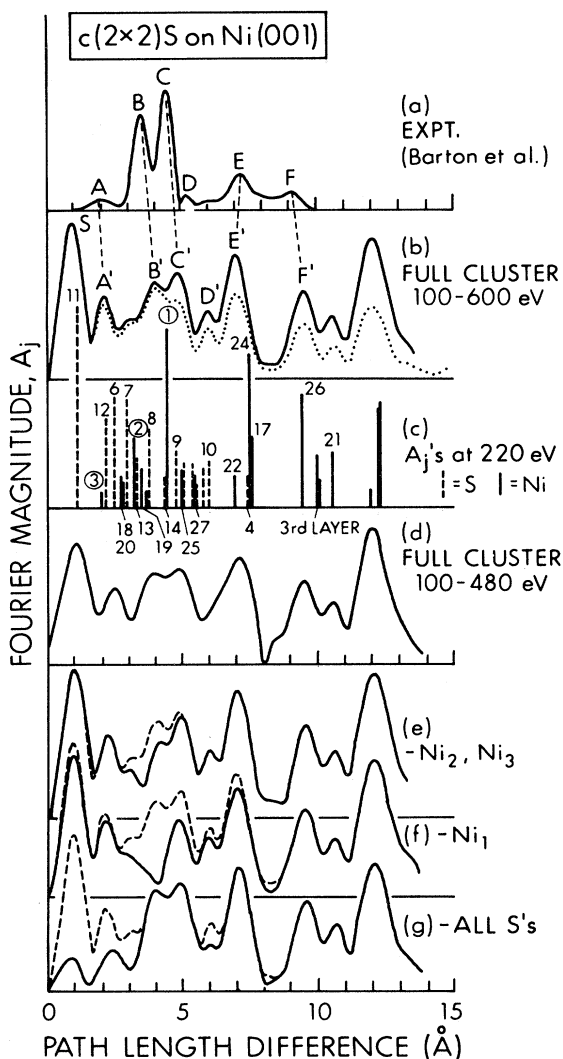


FIG. 3. Fourier transforms of OPD  $\chi(E)$  curves for  $c(2 \times 2)$ S on Ni(001): (a) autoregressive experimental FT of Barton *et al.* (Ref. 3); (b) FT of full-cluster theory over 100–600 eV, with the dotted curve corresponding to a reduction of the inelastic attenuation length by a factor of  $\frac{1}{2}$ ; (c) scattering amplitudes  $A_j$  at 220 eV for most important atoms, with dashed lines being S and solid lines Ni; (d) FT of full cluster over smaller range of 100–480 eV; (e) FT of full cluster minus  $Ni_2$  and  $Ni_3$  atoms; (f) FT of full cluster minus  $Ni_1$  atom; and (g) FT of full cluster minus all S atoms. In (c),  $A_j$ 's without numbers are for atoms outside of the small cluster of Fig. 1. In (e)–(f) the FT range is 100–600 eV, and the dashed curve represents the full-cluster result of (a).

labeled  $A$ ,  $B$ , and  $C$  in Fig. 3 as being directly associated with PLD's to nearest-neighbor nickel atoms of types  $Ni_3$ ,  $Ni_2$ , and  $Ni_1$ , respectively (cf. Fig. 1), and so have suggested that a very direct structural determination can be made. In this paper, we analyze these data in terms of the SSC model used previously in NPD<sup>4</sup> and show that the FT features found are also, in general, not capable of simple interpretation in terms of single PLD's.

The assumptions, basic equations, and input parameters of the SSC model as appropriate to S on Ni are discussed elsewhere.<sup>4,6</sup> The  $\chi(E)$  curve is predicted to be given by

$$\chi(E) \propto \sum_j \frac{A_j(k)}{A_0} \cos[kr_j(1 - \cos\theta_j) + \psi_j(\theta_j, k) + \Phi], \quad (1)$$

in which  $A_0$  is the primary wave amplitude;  $A_j(k)$  is a scattered wave amplitude including factors for the polarization dependence of the dipole matrix element, the scattering factor amplitude, Debye-Waller vibrational attenuation, and inelastic scattering;  $k$  is the electron wave-vector amplitude;  $r_j$  is the distance to scatterer  $j$ ;  $\theta_j$  is the  $j$ -atom scattering angle;  $\psi_j(\theta_j, k)$  is the scattering phase shift; and  $\Phi$  allows for matrix-element-associated parity changes between primary and scattered waves. The quantity  $r_j(1 - \cos\theta_j)$  is the PLD for scatterer  $j$  and a Fourier transform of Eq. (1) as  $\chi(k)$  should thus most simply yield peaks at the PLD's of the strongest scatterers.<sup>4</sup> To insure full convergence, the cluster sum  $j$  was over  $\sim 60$  [for  $p(2 \times 2)$ ] to 120 [for  $c(2 \times 2)$ ] S atoms and  $\sim 1800$  Ni atoms in eight underlying layers; however, a total cluster of as small as  $\sim 100$  atoms was found to yield most of the fully converged features in  $\chi(E)$  and its FT. Angular averaging over a cone of  $\pm 2.3^\circ$  half angle was also carried out to simulate experimental resolution.<sup>3</sup>

In Fig. 2, we compare experimental and theoretical  $\chi(E)$  curves for  $c(2 \times 2)$ S on Ni with different types of clusters in order to determine the degree of influence of certain important classes of atoms. In all of these calculations, S is assumed to be 1.35 Å above the Ni surface.<sup>5</sup> As noted previously for NPD,<sup>4</sup> the full-cluster  $\chi(E)$  curve is found to reproduce the experimental peaks reasonably well, with almost all major features showing correspondence between the two curves. Removing the three nearest neighbors to the sulfur emitter of types  $Ni_2$  and  $Ni_3$  affects the  $\chi(E)$  curve very little, and immediately suggests that these are not major scatterers in the overall cluster. Removing only the nearest-neighbor  $Ni_1$  which has been selected for emphasis by the experimental geometry produces much more noticeable changes in  $\chi(E)$ , for example, in the depth of the minimum for  $\sim 125$ – $150$  eV and the peak shape near 180–225 eV. All of these changes occur in the region from  $\sim 100$ – $300$  eV for which backscattering is strongest.<sup>4</sup> Finally, removing all of the adsorbate atoms from the cluster yields very nearly the same degree of change in  $\chi(E)$  as removing  $Ni_1$ , again principally over  $\sim 100$ – $300$  eV; these results clearly indicate that adsorbates are important scatterers.

The corresponding FT's for  $c(2 \times 2)$ S on Ni(001) are shown in Fig. 3. These are found to be much more sensitive indicators of the effects of different scatterers. The full-cluster FT in Fig. 3(b) as obtained over a broad range of 100–600 eV shows very good correspondence with all of the major features in the experimental FT, with positions of  $A = 2.0$  Å vs  $A' = 2.1$  Å,  $B = 3.5$  Å vs  $B' = 4.0$  Å,  $C = 4.4$  Å vs  $C' = 4.9$  Å,  $E = 7.2$  Å vs  $E' = 7.0$  Å, and  $F = 9.1$  Å vs  $F' = 9.6$  Å; this gives a maximum  $\Delta(\text{PLD})$  of 0.5 Å and an average  $\Delta(\text{PLD})$  of 0.4 Å. The weak feature  $D$  at 5.1 Å also may correspond with  $D'$  at 6.0 Å, although the shift in the effective PLD is larger. As shown below, the strong theoretical peak labeled  $S$  at a very small PLD of 1.0 Å is due to a nearest-neighbor S atom of type  $S_{11}$ , and would be difficult to see experimentally due to its very long wavelength in  $\chi(E)$  and the usual procedure of subtracting off a polynomial in analyzing such data.<sup>3</sup> Although peaks  $E'$  and  $F'$  are too strong in the theoretical curve, this can be

due to any of several factors such as an inadequate degree of inelastic attenuation in the  $A_j$ 's that should suppress peaks at large PLD's to a greater degree [cf. dotted curve in Fig. 3(b)] and/or effects of multiple scattering along the longer paths involved.<sup>7</sup>

The origin of peak  $S$  and certain others in the FT can be directly seen via a vertical line plot of  $A_j(k)$  values versus the PLD,<sup>4</sup> as shown in Fig. 3(c). In this plot, only the  $\sim 30$  strongest atoms are shown. Whenever possible, these are numbered according to Fig. 1. An energy of 220 eV was chosen for this plot to emphasize backscattering from the Ni substrate.<sup>4</sup> At higher energies of 350 and 500 eV, it is found that all nearest-neighbor Ni atoms (that is, of types  $Ni_1$ ,  $Ni_2$ ,  $Ni_3$ ) decrease markedly in relative importance as scatterers in comparison with both S atoms and a number of other Ni atoms of comparable PLD. It is not surprising that S atoms can have large  $A_j$  values, since forward-scattering angles of  $\theta_j \geq 45^\circ$  are involved. From the 220-eV  $A_j$  plot, it is evident that peak  $S$  is due to scattering from  $S_{11}$  just in front of the emitter as viewed from the detection direction. It is also very clear that adsorbates  $S_{6-13}$  are strong scatterers in the PLD region of  $\sim 1.0$ – $6.0$  Å. Of the four Ni atoms that are nearest neighbors to the emitter, only  $Ni_1$  has an overall scattering amplitude  $A_j$  significantly larger than those of the several adsorbates and Ni atoms near it in the PLD, and even this ceases to be true by 500 eV as the relative backscattering strength decreases. There are also a number of Ni scatterers in the 3–6-Å region (e.g.,  $Ni_{18-20}$  and others not labeled or not shown as a result of low  $A_j$  values) whose integrated effects could be significant in producing the resultant FT peaks here. This we explore further below. Aside from peak  $S$ , only peaks  $E'$  and  $F'$  emerge as clearly dominated by 1–2 unique PLD's over the entire FT range: peak  $E'$  by atoms  $Ni_{17}$  and  $N_{24}$  and peak  $F'$  by  $Ni_{26}$  and a third-layer Ni directly below  $Ni_1$ .

A further important question is the influence of the FT energy range on peak intensities and positions. Figure 3(d) illustrates this for a reduced range of 100–480 eV comparable in magnitude with that of the raw experimental data.<sup>3</sup> As expected with a shorter range, all features are broadened relative to Fig. 3(b). The region from 2.5–6.5 Å shows loss of fine structure, and the peaks  $S$  and  $A'$  shift by 0.2 and 0.4 Å, respectively, in position. Narrowing the FT range even further produces larger peak distortions and shifts, with only  $E'$  and  $F'$  remaining stable in position. Thus, even though autoregressive methods have been used to extend the effective experimental data range by approximately two times before Fourier transforming,<sup>3</sup> it seems clear that the range selected may be a sensitive nonstructural variable in such analyses.

We now consider in Figs. 3(e)–3(g) the influence on full-cluster FT's of removing selected types of atoms. Figure 3(e) shows the influence of removing the three nearest-neighbor Ni atoms of types  $Ni_2$  and  $Ni_3$ : The FT is little changed except to slightly reduce the magnitudes for  $\sim 3.0$ – $5.0$  Å, especially that of feature  $B'$ . Separate removal of  $Ni_2$  and  $Ni_3$  atoms also verifies that  $Ni_3$  has almost no influence on the FT, as expected from its low  $A_j$  value. Figure 3(f) shows the effect of removing the backscattering

nearest-neighbor  $Ni_1$ , which is to reduce the intensity of both features  $B'$  and  $C'$ , but primarily that of feature  $B'$  at 4.0 Å, which is almost eliminated. The unique association of atom  $Ni_1$  with feature  $C$  in the experimental FT primarily on the basis of matching PLD's of  $\sim 4.4$  Å thus seems specious. (These effects of removing  $Ni_2$ ,  $Ni_3$ , or  $Ni_1$  on FT's are furthermore found to be essentially identical even in the complete absence of adsorbate scatterers; thus our conclusions are not dependent upon knowing the S relative scattering strength precisely.) Finally, Fig. 3(g) shows the effect of removing all S atoms, and it is clear that this causes dramatic changes in the FT in the region 0–3 Å, and minor changes in 5.5–6.5 Å. Peaks  $B'$  and  $C'$  are, however, very little changed by removing sulfur, suggesting that the S relative phases over 3.5–5.5 Å tend to cause a net cancellation in the FT.<sup>4</sup> As a result of a detailed analysis of all of the  $A_j$ 's involved,<sup>8</sup> we conclude that peaks  $A'$ ,  $B'$ , and  $C'$  are a complex mixture of several Ni and S scatterers. In peak  $A'$ , sulfur plays a strong role. For peak  $B'$ , atom  $Ni_1$  is dominant and  $Ni_2$  atoms play a lesser role. Peak  $C'$  is by contrast less strongly dominated by  $Ni_1$  and must involve other scatterers such as  $Ni_{25}$ ,  $Ni_{27}$ , and a number of other less strongly scattering Ni atoms at approximately the same PLD. By contrast, peaks  $S$ ,  $E'$ , and  $F'$  are found to be simply associated with certain scatterers: removing atom  $S_{11}$  deletes only peak  $S$  in the FT, removing atoms  $Ni_{24}$  and  $Ni_{17}$  deletes only peak  $E'$ , and removing  $Ni_{26}$  and the third-layer atom near it in the PLD deletes only peak  $F'$ .

We have also carried out an identical SSC analysis<sup>8</sup> of the  $\chi(E)$  and FT curves for  $p(2 \times 2)S$  on Cu(001), assuming a  $z$  value of 1.39 Å.<sup>3</sup> This analysis yields the same conclusions as for Ni, although the  $p(2 \times 2)$  overlayer is half as dense and the altered polarization direction of  $\theta_{hv} = 30^\circ$  yields stronger adsorbate scattering per atom.

In conclusion, single-scattering cluster calculations are shown to provide a good description of off-normal photoelectron diffraction data for  $c(2 \times 2)S$  on Ni(001) and  $p(2 \times 2)S$  on Cu(001). An analysis of these SSC calculations and their Fourier transforms also shows that it is not possible to simply associate FT peaks in the  $\sim 2$ – $5$ -Å range with the nearest-neighbor Ni or Cu atoms to the emitter, although two peaks at longer path-length differences of  $\sim 7$  and 9–10 Å can be directly related to pairs of Ni or Cu atoms having nearly identical PLD's. Overall, this study suggests limitations on the use of FT's in OPD structural analyses: FT peaks generally involve more than one strong scatterer (and perhaps many scatterers) and all scatterers must be accurately included in analyzing data for a given adsorption and photoemission geometry.

#### ACKNOWLEDGMENTS

We are indebted to J. J. Barton, D. A. Shirley, and Z. Hussain for providing us with results prior to publication, and for helpful comments. This work was supported by the National Science Foundation under Grant No. CHE80-21355.

\*Present address: Institut für Physik, Technische Universität München, Garching b. München, Federal Republic of Germany.

- <sup>1</sup>D. H. Rosenblatt *et al.*, Phys. Rev. B 26, 1812 (1982), and references therein.
- <sup>2</sup>D. H. Rosenblatt *et al.*, Phys. Rev. B 26, 3181 (1982), and references therein.
- <sup>3</sup>J. J. Barton, C. C. Bahr, Z. Hussain, S. W. Robey, J. G. Tobin, L. E. Klebanoff, and D. A. Shirley, Phys. Rev. Lett. 51, 272 (1983); and (private communication).
- <sup>4</sup>P. J. Orders and C. S. Fadley, Phys. Rev. B 27, 781 (1983).
- <sup>5</sup>S. Brennan, J. Stöhr, and R. Jaeger, Phys. Rev. B 24, 4871 (1981), and references therein.
- <sup>6</sup>P. J. Orders, R. E. Connelly, N. F. T. Hall, and C. S. Fadley, Phys. Rev. B 24, 6163 (1981).
- <sup>7</sup>C. A. Ashley and S. Doniach, Phys. Rev. B 11, 1279 (1975).
- <sup>8</sup>E. Bullock, C. S. Fadley, and P. J. Orders (unpublished).